

Article

Interaction of MdWRKY24 and MdRGL in Response to Tree Dwarfing in *Malus domestica*

He Zhang ¹, Zhichang Yang ¹, Jianzhu Shao ¹, Jianshe Sun ¹, Qian Zha ^{2,*}  and Xueying Zhang ^{1,*}¹ College of Horticulture, Hebei Agricultural University, Baoding 071001, China² Research Institute of Forestry and Pomology, Shanghai Academy of Agricultural Sciences, Shanghai 201403, China

* Correspondence: zhaqian1988@163.com (Q.Z.); zhangxueying1996@163.com (X.Z.)

Abstract: In apple cultivation, dwarf rootstocks are chosen for dense planting and intensive cultivation, which is beneficial to production management. Dwarf rootstocks are widely used in apple production in China. However, the dwarfing mechanisms of dwarf interstock are still unclear. Here, M9 and SH40 were selected as the dwarf interstocks for potted Fuji apples. The key transcription factor MdWRKY24 was screened via transcriptional sequencing. The open reading frame sequence of the *MdWRKY24* gene was 657 bp in length, encoded 218 amino acids, and was located on the cell membrane. The *MdWRKY24*-overexpressing *Arabidopsis* line showed a dwarf phenotype and delayed flowering. The DELLA protein RGA-like (RGL) gene is a repressor of the gibberellin signaling pathway. Yeast two-hybrid analysis revealed that *MdWRKY24* could interact with *MdRGL1/2/3*. The results indicated that *MdWRKY24* might affect plant dwarfing through the synergistic effect of *MdRGL1/2/3*. The *MdWRKY24*-*MdRGL* may be an important pathway underlying the gibberellin-mediated regulation of apple dwarfing.



Citation: Zhang, H.; Yang, Z.; Shao, J.; Sun, J.; Zha, Q.; Zhang, X. Interaction of *MdWRKY24* and *MdRGL* in Response to Tree Dwarfing in *Malus domestica*. *Agronomy* **2022**, *12*, 2345. <https://doi.org/10.3390/agronomy12102345>

Academic Editors: Ali Raza and Aiping Song

Received: 11 August 2022

Accepted: 25 September 2022

Published: 28 September 2022

Publisher's Note: MDPI stays neutral with regard to jurisdictional claims in published maps and institutional affiliations.



Copyright: © 2022 by the authors. Licensee MDPI, Basel, Switzerland. This article is an open access article distributed under the terms and conditions of the Creative Commons Attribution (CC BY) license (<https://creativecommons.org/licenses/by/4.0/>).

Keywords: apple; dwarf; RNA-seq; *MdWRKY24*; *MdRGL*; *Malus domestica*; Fuji; Baleng Crab; *Arabidopsis thaliana*

1. Introduction

Typically, apple cultivation involves the intensive cultivation of dwarf rootstocks with high-density planting. Dwarf rootstocks with high-density planting due to a reduction in tree size, the facilitation of crop management practices, an increase in land use efficiency, and early flowering and fruiting could lead to an increase in profits [1]. In apple cultivation, rootstocks are classified into the following four categories according to tree height and the scion meridian: dwarf, semi-dwarf, intermediate, and vigorous [2,3]. The M9 is a dwarfing rootstock that belongs to the British M series, and the canopy of the scion varieties grafted on them are ca. 50% smaller compared to other standard rootstocks [4]. The SH series rootstocks were selected and bred after 16 years of research (1978–1993) by crossing Guoguang × Henan Begonia by the Fruit Tree Research Institute of the Shanxi Academy of Agricultural Sciences in China. The SH40 is a semi-dwarfing rootstock with a good cold tolerance and is widely used in northern China, and the canopy of the scion varieties grafted on them are ca. 70% smaller compared to other standard rootstock. [5,6]. The application of apple dwarfing rootstock mainly includes rootstock and interstock. In China, the SH series is basically used as an interstock due to its environmental adaptability and difficult rooting and reproduction [7,8].

Transcription factors (TFs) can specifically bind to W-box cis-acting elements on target gene promoters, thereby regulating the target gene expression. Recent studies have shown that WRKY, AP2/EREBP, bHLH, C2H2, NAC, and ARF TFs regulate plant growth and cause dwarfing. WRKY TFs represent one of the most abundant TF families unique to plants discovered in the past 20 years [9]. WRKY TFs in apple [10], tomato [11], and

rice [12] have been identified in genome-wide analyses and the results suggest that they could play multiple roles. WRKY TFs participate in plant growth and development through self-regulation or by regulating downstream hormones and the related pathways [13].

WRKY TFs play important regulatory roles in the growth and development of many plants. Imran et al. [14] reported that AtWRKY62 negatively affects *Arabidopsis* growth. Abeysinghe et al. (2019) obtained a transgenic dwarf phenotype of *Arabidopsis* tetraploids by transforming the AtWRKY18 overexpression vector [15]. Chen et al. [16] reported that CsWRKY7 might participate in plant growth through flowering in tea trees. Zhang et al. [17] reported that OsWRKY78 regulates rice stem elongation and seed development. Zhao et al. [18] ectopically expressed MdWRKY31 in *Arabidopsis* and tobacco and found that MdWRKY31 overexpression increased the sensitivity of apple roots and apple callus to abscisic acid (ABA). In the apple dwarf rootstock M26, MdWRKY9 can inhibit the expression of the brassinolide synthesis gene, eventually causing plant dwarfing [19]. These findings provide strong evidence for the regulation of TFs to cause dwarfing in apple dwarfing rootstocks.

This study focused on the utilization mode (interstock) of apple production to evaluate the effect of SH40 and M9 on the scion. This study aimed to analyze the regulatory mechanism underlying dwarfing under this utilization mode, providing a reference for the early screening and evaluation of interstock selection and cultivation measures for apple growth regulation. It is anticipated that apple dwarfing is governed by a complex multi-gene regulatory mechanism closely related to gene expression regulation by the TFs. Nonetheless, the detailed metabolic regulatory network remains unclear and warrants further in-depth study.

2. Materials and Methods

2.1. Plant Materials

The test materials were 2-year-old Fuji/M9/Mr, Fuji/SH40/Mr, and Fuji/Mr/Mr. All test materials were potted in plastic pots with a diameter of 35 cm and a height of 40 cm, planted using washed river sand as the matrix, and cultivated in a greenhouse. The temperature was 18 ± 2 °C. The daily light–dark irradiation period was set to 16 h/8 h, with a photon flux density of $200 \mu\text{mol}/\text{m}^2 \cdot \text{s}$. The test materials of different stock and scion combinations were cultured using Hoagland's complete nutrient drip irrigation.

The shoot tips and new shoot phloems of different stock combinations were collected in the autumn shoot growth period in late August. The single plant plot was repeated three times. After collection, the samples were wrapped in tin foil, quickly frozen in liquid nitrogen, and stored in a -80 °C refrigerator for later use.

2.2. Extraction of Plant Total RNA and cDNA Synthesis

The total RNA was extracted using the Plant RNA Kit (Tiangen, Beijing, China). The concentration of each RNA sample was determined using NanoDrop 2000 (Thermo Fisher Scientific, Waltham, MA, USA) and $1 \mu\text{g}$ RNA was used to obtain the first-strand cDNA by reverse transcription with the PrimeScriptTM RT Reagent Kit with gDNA Erase (TransGen Biotech, Beijing, China).

2.3. RNA-seq and Enrichment Analysis

The RNA integrity was evaluated on the Agilent 2100 Bioanalyzer (Agilent Technologies, Santa Clara, CA, USA) and samples with an RNA integrity number (RIN) ≥ 7 were used in subsequent analyses. Equal amounts of RNA from shoot tips and new shoot phloems were used to produce cDNA libraries using the TruSeq Stranded mRNA LTSample Prep Kit (Illumina Inc., San Diego, CA, USA). These libraries were then sequenced using the Illumina HiSeq 2500 sequencing platform, and 125–150-bp paired-end reads were generated.

The RNA-seq and data collection were performed by Novogene Co., Ltd. (Beijing, China; reference genome link: http://ftp.ncbi.nlm.nih.gov/genomes/all/GCF_00014876.5.1_MalDomGD1.0/; 21 September 2020). The processed data set was deposited in the

National Center for Biotechnology Information Sequence Read Archive (<http://www.ncbi.nlm.nih.gov/sra/>; 12 June 2022) under the accession number PRJNA848419.

For the transcript-level quantification, the FPKM and read count values of each transcript (protein coding) were calculated using bowtie2 [20] and eXpress [21]. The DEGs were identified using the DESeq functions estimateSizeFactors and nbinomTest [22]. Significantly differential expression was defined as p -value < 0.05 and a fold-change > 2 or < 0.5 . The hierarchical cluster analysis of the DEGs was performed to explore the transcript expression patterns. Gene Ontology (GO) enrichment analyses of the DEGs were performed using Goseq software [23].

2.4. Quantitative Real-Time PCR

The primer sequences used to amplify the genes related to heat stress by quantitative real-time PCR (qRT-PCR) analysis are shown in Table S1. The qRT-PCR analyses were performed on a Roche LC480 device (Roche Diagnostics GmbH, Mannheim, Germany), and fluorescence quantification was carried out using a TransStart Top Green qPCR Super-Mix (TransGen Biotech, Beijing, China). We initially used a two-step PCR amplification procedure, with pre-denaturation at 95 °C for 30 s, followed by 40 cycles of denaturation at 95 °C for 5 s and annealing at 60 °C for 34 s. The amplification, dissolution, and standard curves were automatically generated by the Roche LC480 software. To calculate the gene expression level, we used the $2^{-\Delta\Delta CT}$ method. The relative expression levels of candidate genes were calculated using the β -actin gene product as the template of the internal reference gene standard, and the average ΔCT value of the group with Mr as the interstock was calculated. Each procedure was conducted using three biological replicates.

2.5. Gene Cloning

The full-length ORFs of *MdWRKY24* were retrieved and cloned by transcript BLAST with the Genome Database Rosaceae (GDR) data (<https://www.rosaceae.org/>; 10 October 2020). The primers used were *MdWRKY24*-MF/MR (Table S1). The PCR detection validation was performed using universal primers M13-47/48. The sequences were compared using DNAMAN (Lynnon Biosoft, San Ramon, CA, USA), aligned using ClustalW, and analyzed using MEGA version 7.0 [24].

2.6. Subcellular Localization

The subcellular localization expression vector was pCAMBIA2300:eGFP, and the primers used were *MdWRKY24*-F1/R1. The subcellular localization expression vector pCAMBIA2300:*MdWRKY24*:eGFP was constructed using the Kpn1/Xba1 enzymes. A heat shock protocol was used to transform *E. coli* DH5 α cells (TransGen Biotech, Beijing, China). Recombinant plasmids were identified by colony PCR and confirmed by sequencing. The constructed vector plasmid was then transferred into *Agrobacterium* GV3101. Finally, *Agrobacterium* suspension was injected into the tobacco seedlings (*Nicotiana rustica* var. *pavonii*). The plants were cultured under low-light conditions for 2 d, after which the injected tobacco leaves were observed and imaged using a confocal microscope (C2-ER; Nikon, Minato City, Japan). The excitation and emission wavelengths of the chloroplast fluorescence signal were 640 and 675 nm, respectively, whereas those of the GFP fluorescent proteins were 488 and 510 nm, respectively.

2.7. Protein and Gene Analysis

The chromosomal location of the gene was determined by aligning the sequences on the NCBI website (<http://www.ncbi.nlm.nih.gov>; 26 October 2020). The phosphorylation sites were predicted using the NetPhos3.1 server (<http://www.cbs.dtu.dk/services/NetPhos/>; 26 October 2020). The secondary structures of proteins were predicted using the SOPMA secondary structure prediction method (https://npsa-prabi.ibcp.fr/cgi-bin/npsa_automat.pl?page=npsa_sopma.html; 26 October 2020). Tertiary structure modeling of the *MdWRKY24* proteins was performed using SWISS-MODEL (<https://swissmodel>.

expasy.org/interactive); the higher the global model quality estimate (GMQE; 0, 1) score, the better the model accuracy. QMN4 was used to evaluate the global and local quality of the model to ensure the overall model reliability. The transmembrane domains were predicted using TMHMM 2.0 (<http://www.cbs.dtu.dk/services/TMHMM-2.0/>; 25 October 2020). The protein signal peptides were predicted using SOSUISignal [25]. The genomic regulatory elements were identified using PlantTFDB [26]. The promoter analysis was performed using PlantCARE (<http://bioinformatics.psb.ugent.be/webtools/plantcare/html/>; 26 October 2020) and the plant transcriptional regulation network data platform (<http://plantregmap.gao-lab.org/>; 26 October 2020).

2.8. *Arabidopsis* Genetic Transformation

The primers used were MdWRKY24-F1/R1. The expression vector for genetic transformation, pCAMBIA2300:MdWRKY24, was constructed using KpnI/XbaI enzymes. The inflorescence dip method was used to transform *Arabidopsis*; positive seedlings were screened using 30 µg/mL of hygromycin 1/2 MS plates and verified by PCR. The sterilized T3 seeds of *Arabidopsis* were evenly planted on MS plates (pH 5.8). The plants were grown in a controlled environment with a relative humidity of 60%, a constant temperature of 20–22 °C, and a 14 h/10 h light/dark cycle; the light intensity was 200 µmol/m²/s.

2.9. Yeast Two-Hybrid Analysis

The nuclear system BD vector was pGBKT7 and the nuclear system AD vector was PGADT7. The gene with the vector linker was cloned using seamless cloning and the vector was recombined in one step. pGBKT7:MdWRKY24 did not have a self-activation phenomenon, so the subsequent screening experiments could be performed.

In this experiment, we found homologous genes in *Arabidopsis thaliana* according to the evolutionary tree relationships. *RGL* and *FT* genes may interact with MdWRKY24, as verified by the experiments.

2.10. Statistical Analysis

The data were processed using Microsoft Excel 2007 (Microsoft Corp., Redmond, WA, USA) and the differences were evaluated using the two-tailed t-tests or Duncan's multiple-range test. A *p*-value < 0.05 was considered statistically significant. * Mean *p*-value < 0.05; ** mean *p*-value < 0.01.

3. Results

3.1. Transcriptomic Analysis

Differentially expressed genes (DEGs; namely, MYB, NAC, and WRKY TFs) in the transcriptome data were screened under the conditions of $|\log_2(\text{fold-change})| > 1$ and *p*-value < 0.05. The pairwise comparisons were performed on the three test materials (M9, M26, and SH40), and the DEGs were obtained by sequencing. Table S2 shows the results of comparing M9 with Baleng Crab (Mr). Thirteen TFs were differentially expressed, eight were upregulated and five were downregulated. All the TFs belonged to ten gene families. Table S3 shows the results of comparing SH40 with Mr. Forty-five TFs were differentially expressed, with nine upregulated and thirty-six downregulated TFs. All the TFs belonged to 20 gene families. Table S4 shows the results of comparing SH40 with M9. Fifty-seven TFs were differentially expressed; among them, twenty were upregulated and thirty-seven were downregulated. All the TFs belonged to 20 gene families. The MdWRKY24 (gene ID: 103417614) was the only common differentially expressed gene in the pooled comparison of the three groups (Figure 1), so the following experiments focused on the WRKY family and the functionality of MdWRKY24.

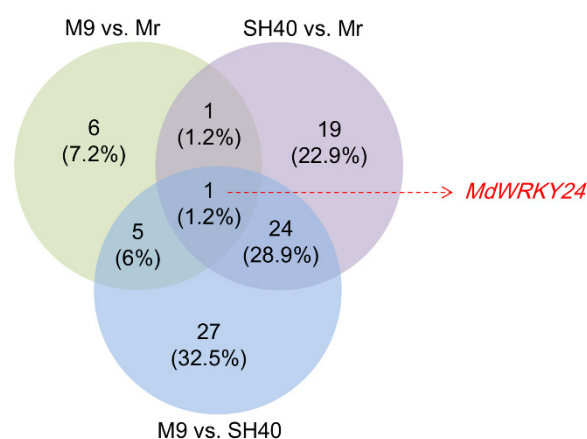


Figure 1. Pairwise comparison of three stock and scion combinations. The numbers of transcription factors with significant differences are indicated in the Venn diagram. M9: Fuji/M9/Mr; SH40: Fuji/SH40/Mr; Mr: Fuji/Mr/Mr. M9 vs. Mr refers to the differences between the means of the three biological replicates of the Fuji/M9/Mr and Fuji/Mr/Mr samples. A similar notation is used for SH40.

3.2. Expression Analysis and GO Enrichment of *MdWRKY* Family Members

By comparing the transcriptome sequencing results in the GDR data, 151 TFs containing conserved WRKY domains were obtained (Table S5). Overall, 125 TFs of the *MdWRKY* family were differentially expressed in different rootstocks (Table S5). Among them, 112, 115, and 120 WRKY TFs were expressed in the groups with SH40, M9, and 120 Mr as the interstock. The selectively expressed genes of the *MdWRKY* family in different stock and scion combinations are shown in Table S6. Gene 103402322 was only expressed in Fuji/SH40/Mr; genes 103402297, 103407769, and 103413747 were not expressed in Fuji/SH40/Mr. Genes 103404419, 103409645, 10341136, 103417041, and 103448476 were only expressed in Fuji/M9/Mr; genes 103411844, 103423637, 103425538, and 103426879 were not expressed only in Fuji/M9/Mr. Genes 103417878, 103425943, 103439393, 103443683, 103450758, and 103451854 were only expressed in Fuji/Mr.

GO enrichment of the 125 differentially expressed WRKY TFs between the three groups with SH40, M9, and Mr as interstocks identified 34 functional categories of biological processes, cellular components, and molecular functions (Figure 2). Among them, more than 100 *MdWRKY* gene family members were enriched in six functional categories, including the cell biological process, biological regulation, metabolic process, biological process regulation, binding function, and nucleic acid-binding TF activity. The first four functional categories (the cellular process, biological regulation, metabolic process, and regulation of biological process) belong to biological processes, and the latter two functional categories (binding and nucleic acid-binding transcription factor activity) belong to molecular functions.

3.3. Analysis of *MdWRKY24*

The *MdWRKY* gene family was screened according to $|\log_2(\text{fold-change})| > 1$ and a p -value < 0.05 . Ten *MdWRKY* TFs were obtained with different interstocks and distributed on different chromosomes (Table 1).

Table 1 shows that *MdWRKY24* expression was significantly upregulated in the scion with M9 as the interstock, compared with the other two groups. The expression of *MdWRKY40*, *MdWRKY70*, *MdWRKY49*, *MdWRKY33*, *MdWRKY50*, and *MdWRKY35* was significantly upregulated in the scion with SH40 as the interstock compared with the other two groups. *MdWRKY7*, *MdWRKY14*, and *MdWRKY13* were significantly downregulated in the scion with SH40 and M9 as the interstock compared to that with Mr as the interstock.

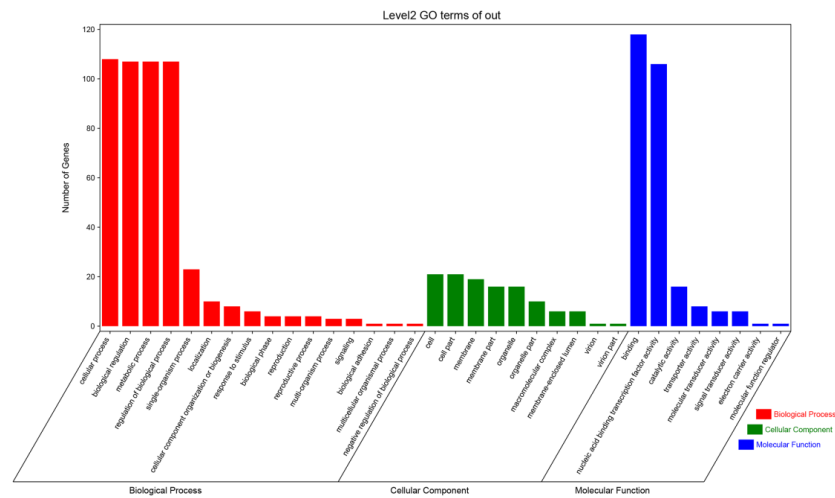


Figure 2. Gene Ontology (GO) enrichment of *MdWRKY* gene family.

Table 1. Significantly differentially expressed *MdWRKY* TFs with different interstocks.

| Gene ID | Gene Name | Chromosome | Fuji/SH40/Mr_FPKM | Fuji/Mr/Mr_FPKM | Fuji/M9/Mr_FPKM |
|-----------|-----------|------------|-------------------|-----------------|-----------------|
| 103421017 | MdWRKY40 | Um | 4.72 | 1.09 | 2.62 |
| 103433764 | MdWRKY70 | 4 | 2.14 | 0.52 | 1.36 |
| 103433503 | MdWRKY49 | 4 | 1.83 | 0.54 | 0.90 |
| 103433719 | MdWRKY33 | 4 | 3.53 | 1.54 | 1.55 |
| 103420177 | MdWRKY50 | 15 | 1.65 | 0.54 | 0.71 |
| 103432616 | MdWRKY35 | 3 | 9.50 | 3.24 | 3.79 |
| 103417614 | MdWRKY24 | 1 | 0.05 | 0.45 | 1.57 |
| 103455944 | MdWRKY7 | 15 | 4.30 | 10.52 | 6.87 |
| 103431032 | MdWRKY14 | 5 | 0.87 | 1.83 | 1.10 |
| 103454203 | MdWRKY13 | 15 | 4.89 | 10.33 | 5.96 |

Note: FPKM, fragments per kilobase per million.

Most *MdWRKY* TFs have a typical WRKYGQK domain, and some core domains are mutated to WRKYGKK. As shown in Figure S1, the amino acid sequences of ten WRKY TFs with significant differences were aligned. Of these, nine WRKY TFs had conserved domains, contained C2H2-type zinc finger structures, and belonged to the WRKY class II subfamily. One protein (gene ID: 103433764) had a conserved WRKY domain, contained a C2HC-type zinc finger structure, and belonged to the WRKY class III subfamily. In the phylogenetic tree of ten significantly differentially expressed TFs, *MdWRKY24* (gene ID: 103417614) and *MdWRKY9* (gene ID: 103433719) were the closest (Figure 3).

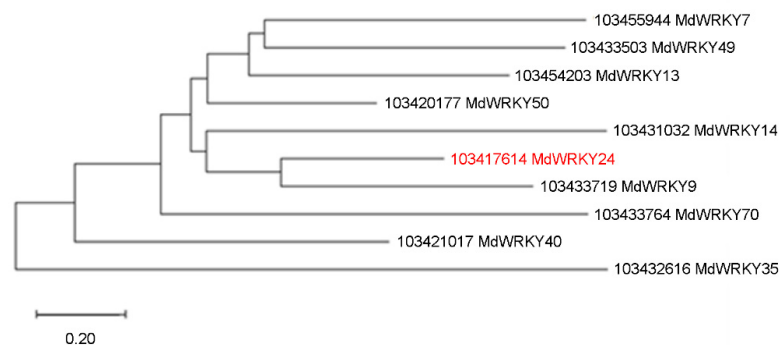


Figure 3. Systematic evolution analysis of ten *MdWRKY* families with significantly differentially expressed genes. The place marked in red is the target gene. The number on a branch represents the frequency parameter for that branch; higher values represent higher confidence.

3.4. Verification of Differential Expression of MdWRKY Transcription Factors

A real-time fluorescence quantification of ten significantly different TFs was performed to verify the reliability of the transcriptome sequencing results (Figure 4). The two methods (qRT-PCR and RNA-seq) had the same overall trend, indicating that the transcriptome sequencing results were reliable and that the follow-up gene screening and experiments could be carried out based on the results.

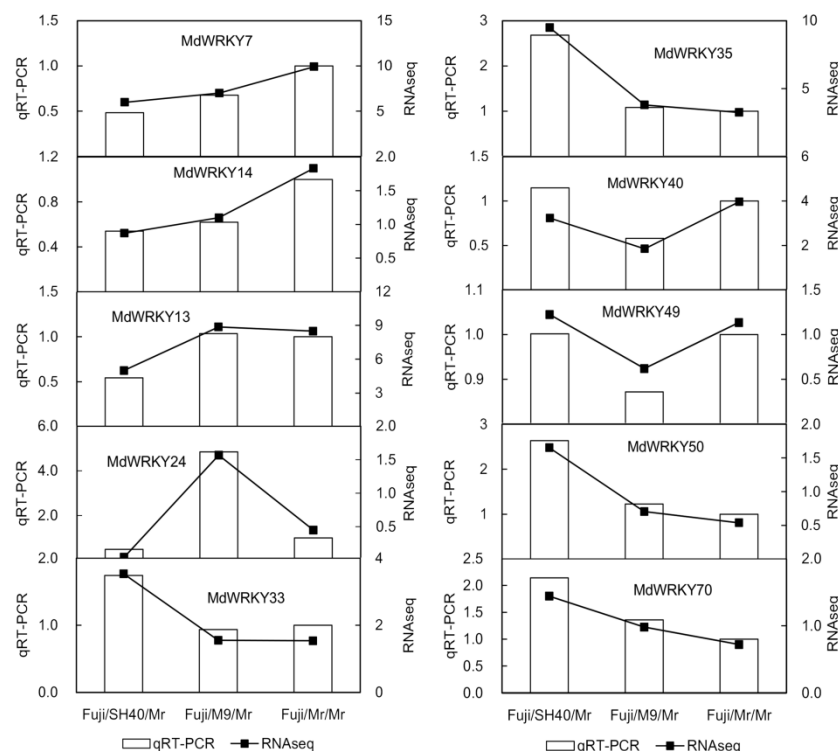


Figure 4. Real-time fluorescence quantitative verification of differentially expressed genes. The bar graph shows the quantitative real-time PCR (qRT-PCR) results, and the line graph shows the expression levels from RNA-seq transcriptome sequencing.

3.5. Bioinformatics Analysis of MdWRKY24

The full-length open reading frame (ORF) region of *MdWRKY24* is 657 bp, encoding 218 amino acids (Figure S2). The *MdWRKY24* phosphorylation sites were analyzed by NetPhos3.1 (Figure 5A). The *MdWRKY24* protein has a total of 43 phosphorylation sites, of which 23 are serine phosphorylation sites, 13 are amino acid phosphorylation sites, and 1 is a tyrosine phosphorylation site, indicating that the phosphorylation modifications of the protein are mainly serine, followed by threonine. The secondary structure of the *MdWRKY24* protein was predicted using SOPMA (Figure 5B). The protein composition consisted of 22.02% α -helix (Hh), 16.51% extended link (Ee), 5.50% β -turn (Tt), and 55.96% random coil (Cc). Figure 5C shows the prediction model of the *MdWRKY24* protein tertiary structure using SWISS-MODEL. The GMQE value of the protein molecular structure encoded by the *MdWRKY24* model was 0.12, the QMN4 value (a comprehensive scoring function for model quality assessment) was -1.22 , the modeling method was X-ray, the resolution was 1.60 Å, and the sequence similarity was 48% (127–200), with a sequence coverage of 34%. The *MdWRKY24* protein is mainly composed of four β -sheets and random coil groups. As shown in Figure 5D, there is no transmembrane helix outside the protein membrane and no transmembrane region, indicating that the *MdWRKY24* protein is an intramembrane protein. Furthermore, *MdWRKY24* was localized in the nucleus (Figure 5E). Figure 5F shows the prediction of the signal peptide of the amino acid sequence of *MdWRKY24* using SignalP5. As no signal peptide was found at the N-terminus of the protein, the *MdWRKY24* gene was presumed to encode a non-secreted protein. Figure 5G

shows the prediction of the MdWRKY24 protein binding motif (T)TGAC (C/T), known as W-box, using PlantTFDB.

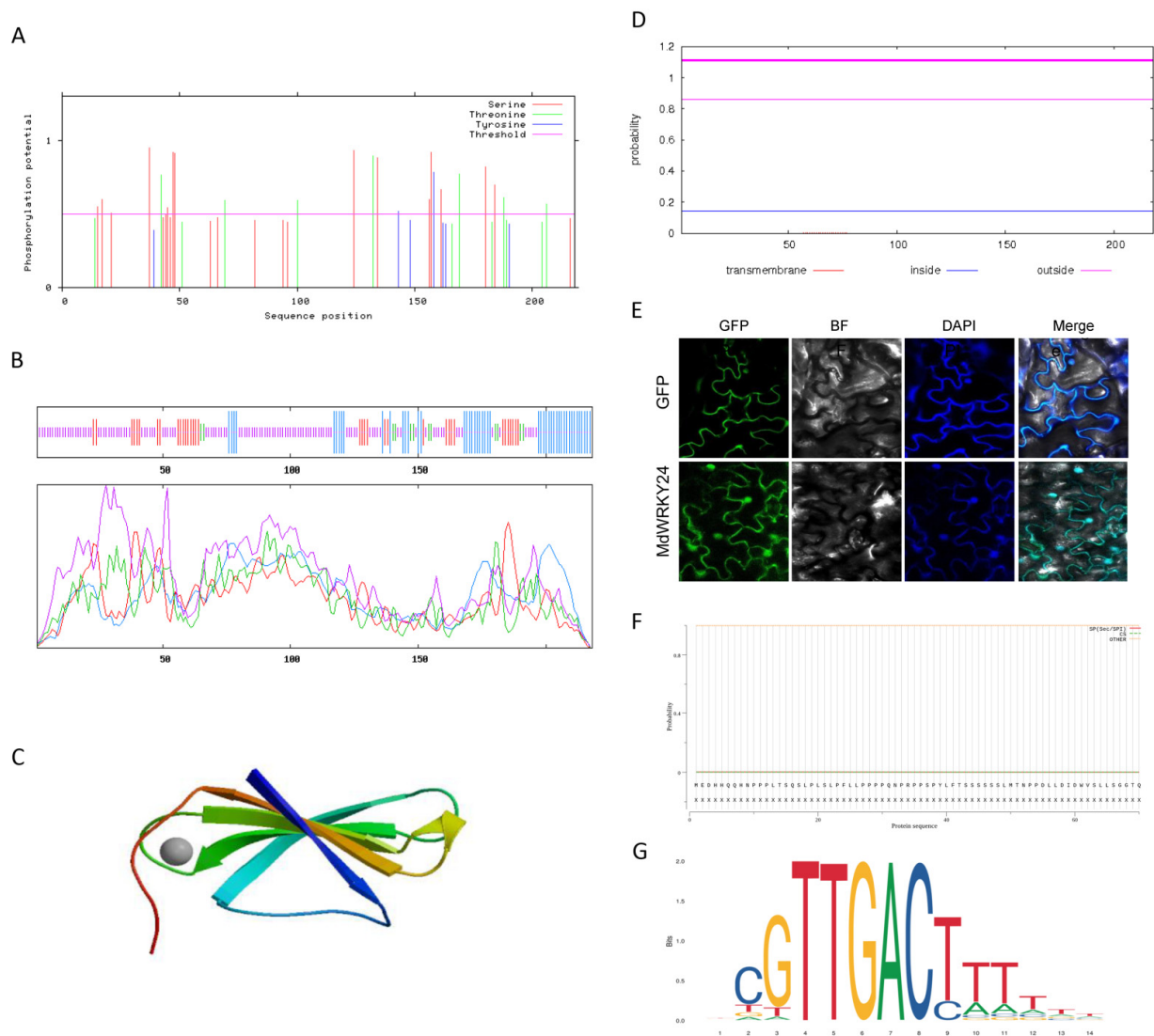


Figure 5. Analysis of MdWRKY24 protein. (A): Phosphorylation sites of MdWRKY24 protein; (B): secondary structure of MdWRKY24 protein. The blue lines represent alpha helices, the red lines represent extended connections, the green lines represent beta turns, and the purple lines represent random coils; (C): tertiary structure of MdWRKY24 protein; (D): MdWRKY24 protein transmembrane structure prediction; (E): subcellular localization of MdWRKY24; (F): signal peptide prediction of MdWRKY24 protein; (G): MdWRKY24 protein binding motif. The letters in the figure indicate the bases, and the sizes of the letters indicate the probability of occurrence.

3.6. Homologous Sequence Alignment and Phylogenetic Tree Analysis of MdWRKY24 Protein

The amino acid sequences of the MdWRKY24 gene were aligned using Blastp. The protein sequences of 14 similar species were obtained, namely white pear (*Pyrus × bretschneideri*), European sweet cherry (*Cerasus avium*), plum (*Armeniaca mume*), peach (*Amygdalus persica*), Tokyo cherry blossom (*Cerasus × yedoensis*), wild strawberry (*Fragaria vesca* ssp.), rose (*Rosa chinensis*), cocoa (*Theobroma cacao*), upland cotton (*Gossypium hirsutum*), longan (*Dimocarpus longan*), *Myrica rubra*, mulberry (*Morus notabilis*), white oak (*Quercus lobata*), and almond (*Amygdalus communis*).

The 15 matched proteins belonged to the WRKY family and contained the WRKY domain, which is a 60-amino acid region defined by the conserved amino acid sequence

WRKYGQK (in the red box) at the N-terminus; they had a novel C2H2-type zinc finger motif (positioned by the black arrow) and belonged to the WRKY class II subfamily (Figure S3). MdWRKY24 binds specifically to the DNA sequence motif (T)(T)TGAC(C/T), known as the W-box. The MdWRKY24 protein highly overlaps with the multiple functional domains of the WRKY proteins of other species (the blue part in the figure). The MdWRKY24 and PbrWRKY24 of white pear were the closest phylogenetically, as they were in the same branch and had the highest protein sequence similarity (Figure 6).

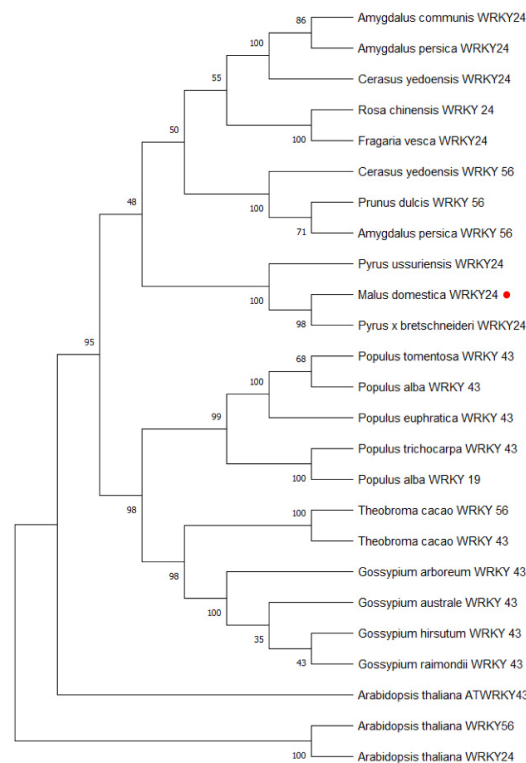


Figure 6. Phylogenetic tree of MdWRKY24 and WRKY proteins of other species. The red dot indicates the MdWRKY24 protein.

3.7. MdWRKY24 Promoter Region Analysis and Upstream Promoter Binding Gene Prediction

In the upstream 1600 bp region of the *MdWRKY24* gene, a number of homeopathic elements or motifs related to plant hormone response were searched, including ABA-related homeopathic elements, ABRE and G-box, methyl jasmonate regulatory motifs, TGACG-motif, and CGTCA-motif (Table 2).

Table 2. Analysis of hormone-related cis-acting elements in the promoter region.

| Motif | Quantity | Function |
|-------------|----------|--|
| ABRE | 1 | ABA response-related cis-acting element |
| G-box | 2 | MeJA/ABA response-related cis-acting element |
| as-1 | 1 | AUXIN response-related cis-acting element |
| GATA-box | 1 | AUXIN response-related cis-acting element |
| CGTCA-motif | 1 | MeJA response-related cis-acting element |
| TGACG-motif | 1 | MeJA response-related cis-acting element |

According to the promoter sequence of the *MdWRKY24* gene and the plant transcriptional regulation network data platform, 21 TFs were predicted to bind upstream, including one AP2 gene family protein, one GATA gene family protein, two BBR_BPC gene family proteins, one C2H2 gene family protein, one GRAS gene family protein, two TALE gene family proteins, two NAC gene family proteins, two MYB related genes family proteins, four

MYB gene family proteins, and five MIKC_MADS gene family proteins. This indicates that the *MdWRKY24* gene may combine with other TFs to regulate downstream target genes.

3.8. Expression of *MdWRKY24* in Different Tissues

As shown in Figure 7, the expression of the *MdWRKY24* gene in the shoot tip and new shoot phloem of the group with M9 as the interstock was significantly higher than that of Fuji/SH40/Mr (about 3 folds) and Fuji/Mr/Mr (1.2–1.5 folds). The expression level of the *MdWRKY24* gene in the phloem of Fuji/Mr/Mr was significantly higher than that of Fuji/SH40/Mr (about 2 folds) and Fuji/M9/Mr (about 3.5 folds).

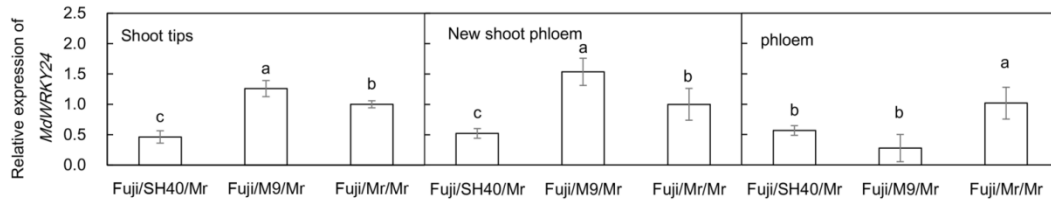


Figure 7. Expression of *MdWRKY24* gene in different parts for the three stock and scion combinations. Lowercase letters indicate significant differences.

3.9. Functional Analysis of *MdWRKY24* after Heterologous Expression in *Arabidopsis*

MdWRKY24 overexpression resulted in dwarfing traits and delayed flowering in *Arabidopsis*. The expression of *AtFT1*, *AtRGL1*, *AtRGL2*, and *AtRGL3* in *MdWRKY24*-overexpressing *Arabidopsis* was significantly lower than that in the wild-type (Figure 8).

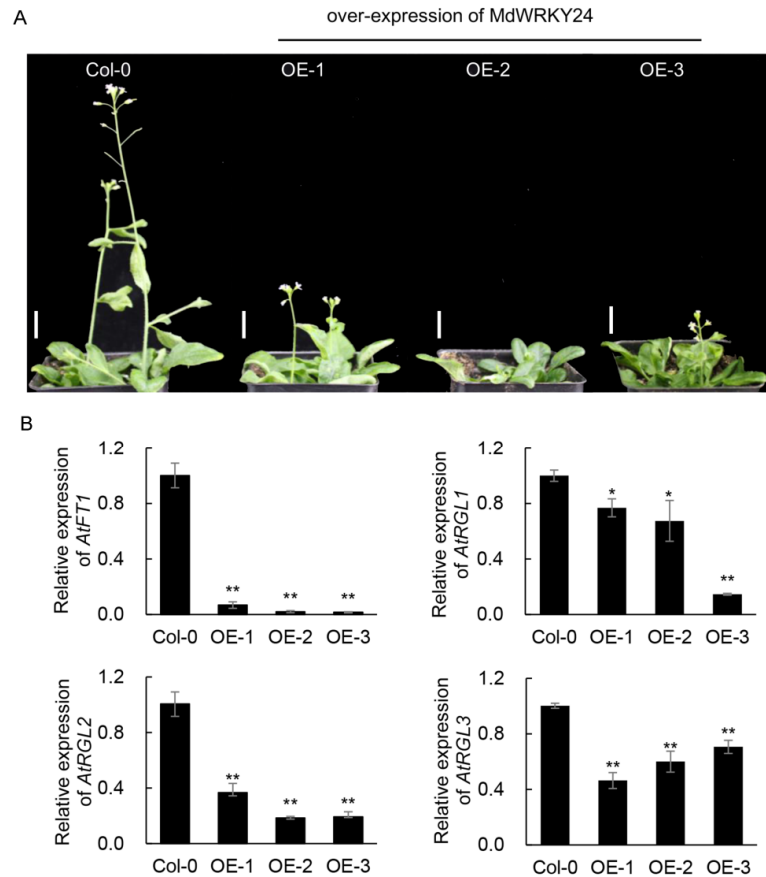


Figure 8. *MdWRKY24* overexpression and qRT-PCR detection of gene expression in transgenic *Arabidopsis*. (A): Phenotype; (B): gene expression. OE-1, OE-2, and OE-3 are *Arabidopsis* overexpression lines. Scale white bar = 2cm. * Mean *p*-value < 0.05; ** mean *p*-value < 0.01.

3.10. Analysis of *MdWRKY24*-Interacting Proteins

MdRGL1-AD+*MdWRKY24*-BD, *MdRGL2*-AD+*MdWRKY24*-BD, and *MdRGL3*-AD+*MdWRKY24*-BD were grown on SD/-Leu/-Trp/-His/-Ade plates (containing X- α -gal), which turned blue; while *MdRGL1*-AD+empty-BD, *MdRGL2*-AD+empty-BD, *MdRGL3*-AD+empty-BD, null-AD+*MdWRKY24*-BD, and *MdFT1*-AD+*MdWRKY24*-BD could not grow on the SD/-Leu/-Trp/-His/-Ade plates (Figure 9). There was no obvious color change on the SD/-Leu/-Trp/-His/-Ade plates (containing X- α -gal). The above results indicate that *MdRGL1*, *MdRGL2*, and *MdRGL3* interact with *MdWRKY24*, but *MdFT1* does not interact with *MdWRKY24*.

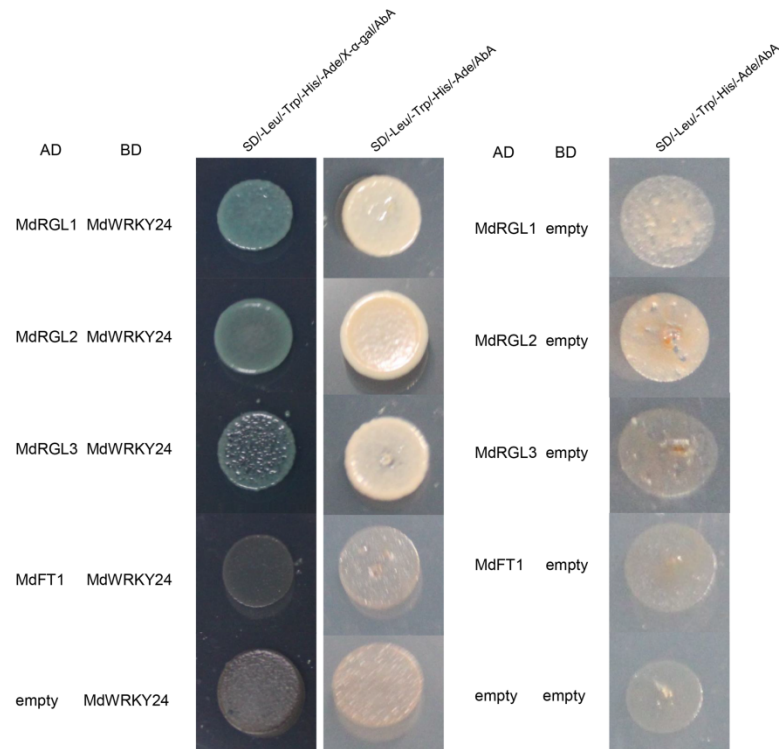


Figure 9. Yeast two-hybrid analysis of the interaction between *MdRGL1*, *MdRGL2*, *MdRGL3*, *MdFT1*, and *MdWRKY24*.

4. Discussion

In the present study, 150 possible WRKY TFs were obtained by analyzing the RNA-seq data. The *MdWRKY* TFs were selectively expressed in different stock and scion combinations. The expression analysis of *MdWRKY24* showed different expression patterns in different stock and scion combinations. Differences between groups were significant, consistent with the trend of differential expression in the shoot tip and new shoot phloem, indicating that the differential regulation of TF expression inherent in rootstocks may yield expression differences in the scion, regulating the growth of the tree.

The pairwise comparison of the WRKY TFs of different stock-scion combinations revealed that the *MdWRKY24* gene was differentially expressed. The CDs sequence of the cloned *MdWRKY24* gene was 657 bp, containing the conserved WRKYGQK domain and the C2H2-type zinc finger structure, thus belonging to the WRKY class II subfamily. The downstream protein binding motif was W-box. *MdWRKY24* had the highest similarity with the *PbrWRKY24* protein in white pear; however, the function of *PbrWRKY24* is still unclear. Phylogenetic tree analysis of apple family members revealed that *MdWRKY24* and *MdWRKY9* were most closely related.

WRKY TFs have a wide range of functions and play important roles in plant growth and stress responses. Previous studies have shown that *MdWRKY9* overexpression in the M26 rootstock can inhibit the expression of the brassinolide synthesis gene *MdDWF4*,

resulting in a decrease in the content of brassinolide in M26 and a dwarf phenotype [19] in *Arabidopsis thaliana*. Analysis of the AtWRKY62 loss-of-function mutants confirmed that AtWRKY62 adversely affected the *Arabidopsis* growth [14]. After the transfection of the AtWRKY18 overexpression vector into the *Arabidopsis* tetraploids, the growth of the transgenic *Arabidopsis* was reduced, and a dwarf phenotype appeared [15]. Here, we noted that dwarfing traits emerged after the MdWRKY24 overexpression, supporting that MdWRKY TFs are related to plant dwarfing. These findings provide strong evidence that the dwarfing-related TFs induced by dwarfing rootstocks regulated growth in apple trees.

MdWRKY45 interacts with the DELLA protein RGA-like 1 (RGL1), a repressor of the gibberellin signaling pathway, and WRKY45, which actively regulates age-induced leaf senescence. RGL1 is a key component of the gibberellic acid (GA)-mediated signaling pathway [27]. Both in vivo and in vitro biochemical analyses demonstrated that WRKY75 interacts with DELLA proteins [28]. We found that both RGL1 and GA insensitive (GAI) inhibited the activation ability of AtWRKY75, thereby attenuating the expression of its regulator [28]. Therefore, we also analyzed the relationship between MdWRKY24 and RGL genes and found that MdWRKY24 and MdRGL1/2/3 can interact, indicating that the MdWRKY24-MdRGL pathway mediates the GA signaling pathway to regulate plant growth and the dwarfing phenotype.

In the present paper, the RGL gene was identified as a DELLA-like protein, metabolized by gibberellin, and related to apple dwarfing. Zhang et al. [29] found that the IAA export protein PIN played a key role in the dwarfing of M9. MdNAC1 plays a role in plant dwarfing traits, potentially by regulating ABA and BR production [30]. The results of the studies above indicate that hormones (gibberellin, IAA, ABA, and BR) are related to the mechanism of dwarfing rootstocks. Therefore, whether the dwarfing traits of plants depend on a single hormone or the synergistic effects of multiple hormones warrants further research.

Chen et al. [16] found that CsWRKY7 may be involved in plant growth in tea plants. They studied the flowering time integrator gene and floral meristem characteristic genes of WRKY7-overexpressing lines. Furthermore, mutations in the AtWRKY75 gene lead to delayed flowering in *Arabidopsis*, and chromatin immunoprecipitation analysis showed that AtWRKY75 directly binds to the promoter of *MdFT1* [28]. Genetic analysis showed that AtWRKY75 positively regulates flowering in a FLOWERING LOCUS T (FT)-dependent manner [28]. Here, we found that MdWRKY24 overexpression delayed flowering, and yeast two-hybrid mining revealed no interaction between MdWRKY24 and the flowering gene *MdFT1*, indicating that MdWRKY24 may affect plant flowering in other ways. TFs regulate the specific spatiotemporal transcription of downstream target genes by binding to specific cis-elements (hormone-related and photosynthetic-related homeopathic elements), thereby precisely regulating the timing of plant development and rapidly responding to external stresses. The present study found that the *MdWRKY24* gene promoter has 21 binding protein motifs for AP2, GATA, BBR_BPC, C2H2, GRAS, TALE, NAC, MYB, and MIKC_MADS TFs. These results indicate that the *MdWRKY24* gene may be mobilized by hormones, photosynthesis, or TFs. Follow-up research should explore more in-depth molecular regulation pathways related to MdWRKY24-mediated regulation of dwarfing mechanisms. Nevertheless, the current study provides a new path for the molecular-assisted breeding of apple dwarf rootstocks, offering technical support for further developing apple cultivation techniques.

Supplementary Materials: The following supporting information can be downloaded at: <https://www.mdpi.com/article/10.3390/agronomy12102345/s1>, Figure S1: sequence alignment of ten *MdWRKY* family genes with significant differences. The black square indicates the conserved domain of *MdWRKY*; the solid line arrow indicates the C2H2-type zinc finger structure; and the dotted line arrow indicates the C2HC-type zinc finger structure. Figure S2: comparison of the *MdWRKY24* gene sequence in different genomes. 103417614 sequencing sequence; XM_008355785.3NCBI genome sequence; MD01G1071600 genome sequence. Figure S3: homologous sequence alignment of MdWRKY24 and WRKY proteins of other species. The red box is amino acid sequences; black arrows

denote zinc finger motifs. Table S1: sequences of primers. Table S2: differentially expressed transcription factors between groups with M9 and Mr as interstocks. Table S3: differentially expressed transcription factors between groups with SH40 and Mr as interstocks. Table S4: differentially expressed transcription factors between groups with SH40 and M9 as interstocks. Table S5: expression of WRKY TF family members in different stock and scion combinations. Table S6: WRKY transcription factors were not expressed in all three rootstock panicle combinations.

Author Contributions: Conceptualization, H.Z.; data curation, formal analysis, validation, methodology, visualization, writing—original draft, Z.Y.; data curation, validation, J.S. (Jianzhu Shao); methodology, J.S. (Jianshe Sun) and X.Z.; formal analysis, Q.Z.; writing—original draft. All authors have read and agreed to the published version of the manuscript.

Funding: This project was supported by the Natural Science Foundation of Hebei Province of China (Grant No. C2020204043) and the Earmarked Fund for Hebei Apple Innovation Team of Modern Agro-industry Technology Research System (HBCT2021100409 and HBCT2021100210).

Data Availability Statement: The clean data set was deposited in the National Center for Biotechnology Information Sequence Read Archive (<http://www.ncbi.nlm.nih.gov/sra/>, accessed on 13 July 2022) under the accession number PRJNA848419.

Acknowledgments: The test materials for dwarf rootstocks were provided by Zhang Xinzong of China Agricultural University.

Conflicts of Interest: The authors declare that the research was conducted in the absence of any commercial or financial relationships that could be construed as a potential conflict of interest.

References

- Xu, X.; Du, X.; Wang, F.; Sha, J.; Chen, Q.; Tian, G.; Zhu, Z.; Ge, S.; Jiang, Y. Effects of potassium levels on plant growth, accumulation and distribution of carbon, and nitrate metabolism in apple dwarf rootstock seedlings. *Front. Plant Sci.* **2020**, *11*, 904. [[CrossRef](#)] [[PubMed](#)]
- Lauri, P.É.; Maguylo, K.; Trottier, C. Architecture and size relations: An essay on the apple (*Malus × domestica*, Rosaceae) tree. *Am. J. Bot.* **2006**, *93*, 357–368. [[CrossRef](#)] [[PubMed](#)]
- Wang, Y.; Li, W.; Xu, X.; Qiu, C.; Wu, T.; Wei, Q.; Ma, F.; Han, Z. Progress of apple rootstock breeding and its use. *Hortic. Plant J.* **2019**, *5*, 183–191. [[CrossRef](#)]
- Pilcher, R.L.R.; Celton, J.M.; Gardiner, S.E.; Tustin, D.S. Genetic markers linked to the dwarfing trait of apple rootstock ‘Malling 9’. *J. Am. Soc. Hortic. Sci.* **2008**, *133*, 100–106. [[CrossRef](#)]
- Marini, R.P.; Fazio, G. Apple rootstocks: History, physiology, management, and breeding. *Hortic. Rev.* **2018**, *45*, 197–312. [[CrossRef](#)]
- Li, X.L.; Zhang, J.K.; Li, M.J.; Zhou, B.B.; Zhang, Q.; Wei, Q.P. Influence of six dwarfing interstocks on the ‘Fuji’ apple under drought stress. *Indian J. Hortic.* **2017**, *74*, 346–350. [[CrossRef](#)]
- Liang, B.; Shi, Y.; Yin, B.; Zhou, S.; Li, Z.; Zhang, X.; Xu, J. Effect of different dwarfing interstocks on the vegetative growth and nitrogen utilization efficiency of apple trees under low-nitrate and drought stress. *Sci. Hortic.* **2022**, *305*, 111369. [[CrossRef](#)]
- Zhang, D.; Li, C.; Zhang, H.; Zhao, J.Z.; Sun, J.S. The tissue anatomy analysis of the temporary planting SH40 interstock apple seedling water loss during the period of dormancy. *J. West China For. Sci.* **2018**, *47*, 91–95. [[CrossRef](#)]
- Xu, R.R.; Zhang, S.Z.; Cao, H.; Shu, H.R. Bioinformatics analysis of WRKY transcription factor genes family in apple. *Acta Hortic. Sin.* **2012**, *39*, 2049. [[CrossRef](#)]
- Zhang, H.; Yang, L.; Zhou, R.; Zhang, Y.; Wang, Z.; Pang, H.; Bai, T.; Song, S.; Jiao, J.; Wang, M.; et al. Genome wide transcriptomic analysis of WRKY gene family response to biotic stresses in *Malus × domestica*. *Am. J. Plant Sci.* **2021**, *12*, 858–885. [[CrossRef](#)]
- Huang, S.; Gao, Y.; Liu, J.; Peng, X.; Niu, X.; Fei, Z.; Cao, S.; Liu, Y. Genome-wide analysis of WRKY transcription factors in solanum Lycopersicum. *Mol. Genet. Genomics* **2012**, *287*, 495–513. [[CrossRef](#)] [[PubMed](#)]
- Ross, C.A.; Liu, Y.; Shen, Q.J. The WRKY gene family in rice (*Oryza sativa*). *J. Integr. Plant Biol.* **2007**, *49*, 827–842. [[CrossRef](#)]
- Jiang, J.; Ma, S.; Ye, N.; Jiang, M.; Cao, J.; Zhang, J. WRKY transcription factors in plant responses to stresses. *J. Integr. Plant Biol.* **2017**, *59*, 86–101. [[CrossRef](#)] [[PubMed](#)]
- Imran, Q.M.; Hussain, A.; Mun, B.G.; Lee, S.U.; Asaf, S.; Ali, M.A.; Lee, I.; Yun, B. Transcriptome wide identification and characterization of NO-responsive WRKY transcription factors in *Arabidopsis thaliana* L. *Environ. Exp. Bot.* **2018**, *148*, 128–143. [[CrossRef](#)]
- Abeyasinghe, J.K.; Lam, K.M.; Ng, D.W.-K. Differential regulation and interaction of homoeologous WRKY 18 and WRKY 40 in *Arabidopsis* allotetraploids and biotic stress responses. *Plant J.* **2019**, *97*, 352–367. [[CrossRef](#)]
- Chen, W.; Hao, W.J.; Xu, Y.X.; Zheng, C.; Ni, D.J.; Yao, M.Z.; Chen, L. Isolation and characterization of CsWRKY7, a subgroup IIInd WRKY transcription factor from *Camellia sinensis*, linked to development in *Arabidopsis*. *Int. J. Mol. Sci.* **2019**, *20*, 2815. [[CrossRef](#)]

17. Zhang, C.Q.; Xu, Y.; Lu, Y.; Yu, H.X.; Gu, M.H.; Liu, Q.Q. The WRKY transcription factor OsWRKY78 regulates stem elongation and seed development in rice. *Planta* **2011**, *234*, 541–554. [[CrossRef](#)]
18. Zhao, X.Y.; Qi, C.H.; Jiang, H.; You, C.X.; Guan, Q.M.; Ma, F.W.; Li, Y.Y.; Hao, Y.J. The MdWRKY31 transcription factor binds to the MdRAV1 promoter to mediate ABA sensitivity. *Hortic. Res.* **2019**, *6*, 66. [[CrossRef](#)]
19. Zheng, X.; Zhao, Y.; Shan, D.; Shi, K.; Wang, L.; Li, Q.; Wang, N.; Zhou, J.; Yao, J.; Xue, Y.; et al. MdWRKY9 overexpression confers intensive dwarfing in the M26 rootstock of apple by directly inhibiting brassinosteroid synthetase MdDWF4 expression. *New Phytol.* **2018**, *217*, 1086–1098. [[CrossRef](#)]
20. Langmead, B.; Salzberg, S.L. Fast gapped-read alignment with bowtie 2. *Nat. Methods* **2012**, *9*, 357–359. [[CrossRef](#)]
21. Roberts, A.; Pachter, L. Streaming fragment assignment for real-time analysis of sequencing experiments. *Nat. Methods* **2013**, *10*, 71–73. [[CrossRef](#)] [[PubMed](#)]
22. Anders, S.; Huber, W. Differential Expression of RNA-Seq Data at the Gene Level—The DESeq Package. 2013. Available online: <http://www.bioconductor.org/packages/devel/bioc/vignettes/DESeq/inst/doc/DESeq.pdf> (accessed on 17 October 2013).
23. Young, M.D.; Wakefield, M.J.; Smyth, G.K.; Oshlack, A. Gene ontology analysis for RNA-seq: Accounting for selection bias. *Genome Biol.* **2010**, *11*, R14. [[CrossRef](#)] [[PubMed](#)]
24. Kumar, S.; Stecher, G.; Tamura, K. MEGA7: Molecular Evolutionary Genetics Analysis Version 7.0 for Bigger Datasets. *Mol. Biol. Evol.* **2016**, *33*, 1870–1874. [[CrossRef](#)]
25. Gomi, M.; Akazawa, F.; Mitaku, S. SOSUIsignal: Software system for prediction of signal peptide and membrane protein. *Genome Inform.* **2000**, *11*, 414–415.
26. Jin, J.; Tian, F.; Yang, D.C.; Meng, Y.Q.; Kong, L.; Luo, J.; Gao, G. PlantTFDB 4.0: Toward a central hub for transcription factors and regulatory interactions in plants. *Nucleic Acids Res.* **2017**, *45*, D1040–D1045. [[CrossRef](#)] [[PubMed](#)]
27. Chen, L.; Xiang, S.; Chen, Y.; Li, D.; Yu, D. Arabidopsis WRKY45 interacts with the DELLA protein RGL1 to positively regulate age-triggered leaf senescence. *Mol. Plant* **2017**, *10*, 1174–1189. [[CrossRef](#)] [[PubMed](#)]
28. Zhang, L.; Chen, L.; Yu, D. Transcription factor WRKY75 interacts with DELLA proteins to affect flowering. *Plant Physiol.* **2018**, *176*, 790–803. [[CrossRef](#)]
29. Zhang, H.; An, H.S.; Wang, Y.; Zhang, X.Z.; Han, Z.H. Low expression of PIN gene family members is involved in triggering the dwarfing effect in M9 interstem but not in M9 rootstock apple trees. *Acta Physiol. Plant* **2015**, *37*, 104. [[CrossRef](#)]
30. Jia, D.; Gong, X.; Li, M.; Li, C.; Sun, T.; Ma, F. Overexpression of a novel apple NAC transcription factor gene, MdNAC1, confers the dwarf phenotype in transgenic apple (*Malus domestica*). *Genes* **2018**, *9*, 229. [[CrossRef](#)]